

ОБЪЕДИНЕННЫЙ  
ИНСТИТУТ  
ЯДЕРНЫХ  
ИССЛЕДОВАНИЙ  
ДУБНА

E1-88-244

180  
P.Kozma, B.Tumendemberel, D.Chultem\*

**NUCLEAR REACTIONS  
OF MEDIUM AND HEAVY TARGET NUCLEI  
WITH HIGH-ENERGY PROJECTILES.**

**Spallation of  $^{55}\text{Mn}$ ,  $^{59}\text{Co}$ ,  $^{\text{nat}}\text{Ni}$  and  $^{\text{nat}}\text{Cu}$   
by 3.65 AGeV  $^{12}\text{C}$ -ions  
and 3.65 GeV Protons**

Submitted to "Czechoslovak Journal of Physics B"

\* Mongolian State University, Ulan Bator, Mongolia

**1988**

## 1. INTRODUCTION

The past decade witnessed particular interest in the experimental study of nuclear reactions induced by high-energy projectiles<sup>/1/</sup>. Such studies yield valuable information not only for understanding the reaction mechanism and nuclear properties, but also for testing the basic concepts of high-energy physics. The interactions of high-energy projectiles with complex nuclei can be understood in terms of a two-step mechanism<sup>/2/</sup> in which the excitation and deexcitation stages are assumed. Experimental data are usually discussed in the framework of two extreme concepts of the mechanism: the intranuclear-cascade evaporation<sup>/3,4/</sup> and the abrasion-ablation<sup>/5/</sup> models. It should be noted that both model representations can be used to calculate the mass distribution of the target-like residues produced in these reactions.

Two hypotheses originally developed to describe nucleus-nucleus interactions<sup>/6/</sup> can be also applied. The hypothesis of limiting fragmentation predicts that the energy spectra and cross sections of a fragment in its proper frame /either a projectile or a target/ should become independent of bombarding energy at sufficiently high energies. The second one, factorization, predicts that both the spectra and yields of a given fragment can be written as a product of a target /or projectile/ factor. The distribution of target fragments is independent of the nature of the projectile, except for a constant term /the ratio of projectile factors/, and vice versa for projectile fragments.

In this context a careful and systematic experimental study of the distribution of target fragments produced in high-energy nuclear reactions is worthwhile. Particularly, it is desirable to investigate the yields of products formed in relativistic heavy-ion interactions with those produced in proton-induced reactions at the same AGeV energy. Using this motivation, we have undertaken a study of the nuclear reactions induced by 3.65 AGeV  $^{12}\text{C}$ -ions and 3.65 GeV protons with medium and heavy target nuclei using the foil stack activation technique and Ge/Li/ gamma-ray spectroscopy. As a first step, the experimental results concerned with the spallation of  $^{55}\text{Mn}$ ,  $^{59}\text{Co}$ ,  $^{\text{nat}}\text{Ni}$  and  $^{\text{nat}}\text{Cu}$  are presented.

## 2. EXPERIMENTAL PROCEDURE

Irradiations were performed using the external beams of 3.65 GeV protons and 3.65 AGeV  $^{12}\text{C}$ -ions at the Dubna synchrophasotron. The irradiation conditions are summarized in Table 1. Each target stack consisted of three foils: the others were used for recoil loss compensation, the central foil was analyzed. The target foils enclosed in the Mylar catchers 17.5 mg/cm<sup>2</sup> thick were preceded on the upstream side by a 19.5 mg/cm<sup>2</sup> aluminium foil surrounded by Al guard foils of the same thicknesses. The induced  $^{24}\text{Na}$  activity in the central Al foil, along with the known<sup>/7/</sup> cross sections for the  $^{27}\text{Al}/^{12}\text{C}, \text{X}/^{24}\text{Na}$  and  $^{27}\text{Al}/\text{p}, \text{X}/^{24}\text{Na}$  reactions of 19.0 mb and 8.3 mb, respectively, was used to calculate the beam flux. The guard aluminium foils were used for recoil activities elimination. The diameters of the target stacks were 4 cm / $^{55}\text{Mn}$ ,  $^{59}\text{Co}$ / and 8 cm / $^{\text{nat}}\text{Ni}$ ,  $^{\text{nat}}\text{Cu}$ /.

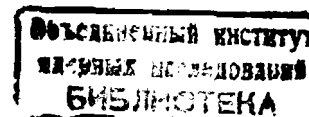


Table 1 Irradiation conditions

Beam	Target	Total flux particles	Target thickness [mg/cm <sup>2</sup> ]
3.65 GeV protons	<sup>55</sup> Mn	5.75x10 <sup>12</sup>	45.2
	<sup>59</sup> Co	8.12x10 <sup>12</sup>	58.5
	nat <sub>Ni</sub>	1.83x10 <sup>13</sup>	31.0
	nat <sub>Cu</sub>	1.47x10 <sup>13</sup>	44.7
3.65 AGeV <sup>12</sup> C-ions	<sup>55</sup> Mn	8.73x10 <sup>11</sup>	45.2
	<sup>59</sup> Co	9.05x10 <sup>11</sup>	58.3
	nat <sub>Ni</sub>	1.76x10 <sup>12</sup>	31.0
	nat <sub>Cu</sub>	2.01x10 <sup>12</sup>	44.9

After irradiation, gamma-rays from target foils and monitors were measured directly with Ge/Li/-detectors. The spectra were recorded with a conventional multichannel system and analyzed by means of computer programs which found all significant peaks and computed their areas and decay rates<sup>/8/</sup>. A typical gamma-ray spectrum from the cobalt target, obtained several hours after proton irradiation, is illustrated in Fig.1. The radioactive nuclides produced in the irradiations were identified by their half-lives, energies and abundances of the emitted gamma-rays. Their relevant properties<sup>/9/</sup> are given in Table 2.

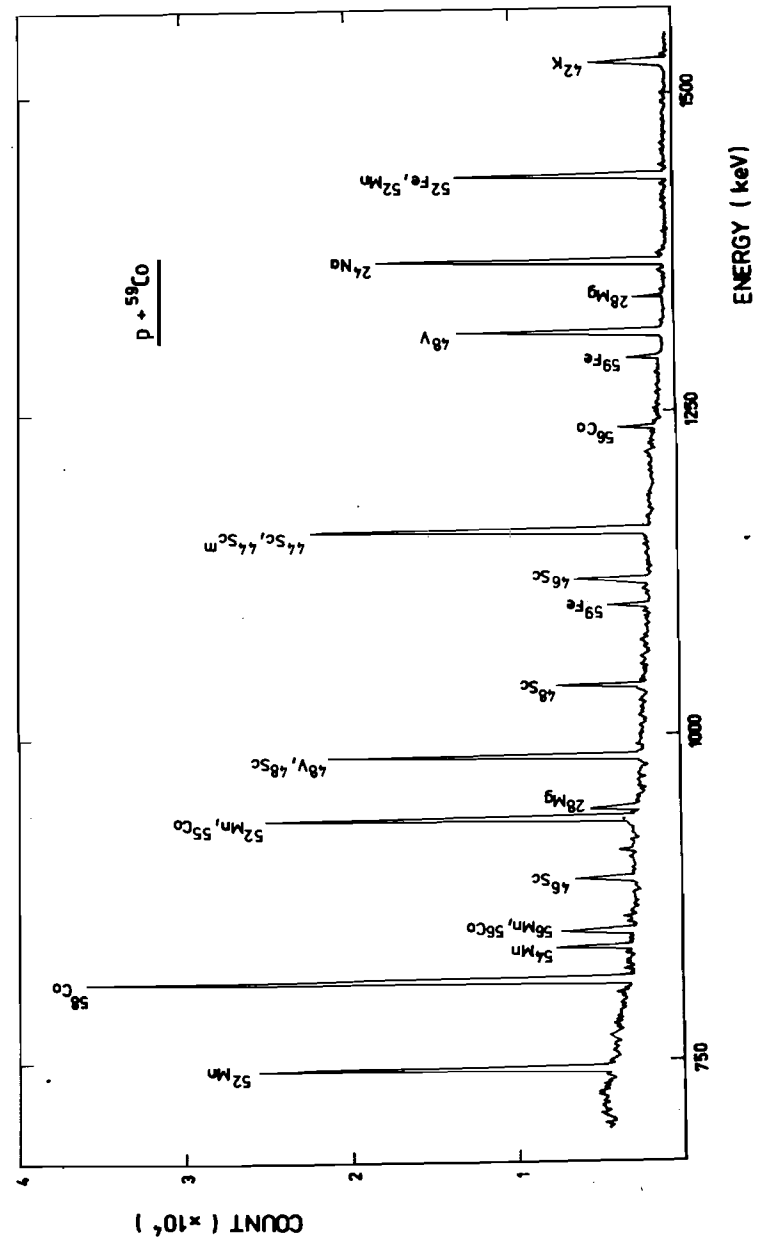


Fig.1. The gamma-ray spectrum of the cobalt target taken with a 45 cm<sup>3</sup> Ge/Li/ - detector several hours after irradiation by 3.65 GeV protons.

Table 2 Relevant properties of the measured nuclides

Nuclide	Half-live	Radiation measured /keV/	Fractional abundance /%/
<sup>65</sup> Zn	244.1 d	1115	50.7
<sup>61</sup> Cu	3.41h	283	13.1
		656	11.2
<sup>57</sup> Ni	36.1 h	1378	77.7
<sup>56</sup> Ni	6.1 d	158	98.8
		812	86.0
<sup>60</sup> Co	5.27y	1173	100
		1333	100
<sup>58</sup> Co	70.9 d	811	99.4
<sup>57</sup> Co	271.8d	122	85.6
<sup>56</sup> Co	78.8 d	847	99.95
<sup>55</sup> Co	17.5 h	1408	16.5
<sup>59</sup> Fe	44.5 h	1099	56.5
<sup>52</sup> Fe	8.27 h	1434	100
<sup>56</sup> Mn	2.58 h	1811	27.3
<sup>54</sup> Mn	312.5 d	835	100
<sup>52</sup> Mn	5.59 d	744	90.0
		1434	100
<sup>51</sup> Cr	27.7 d	320	10.2
<sup>48</sup> Cr	22.96 h	308	100
<sup>48</sup> V	15.97 d	984	100
<sup>48</sup> Sc	43.7 h	1038	97.5
<sup>47</sup> Sc	3.34 d	159	68.5
<sup>46</sup> Sc	83.83 d	889	100
<sup>44</sup> Sc <sup>m</sup>	2.44 d	272	86.6
<sup>44</sup> Sc	3.93 h	1157	99.89
<sup>43</sup> Sc	3.89 h	373	22.5

Table 2 /continued/

Nuclide	Half-live	Radiation measured /keV/	Fractional abundance /%/
<sup>43</sup> K	22.3 h	373	87.8
<sup>42</sup> K	12.36 h	1525	18.8
<sup>28</sup> Mg	20.9 h	1779	100
<sup>24</sup> Na	15.02 h	1369	100

The nuclidic cross sections  $\sigma$  were determined using the standard formula<sup>/10/</sup>

$$\sigma = \frac{N_p A_{gm} \lambda}{\phi W f_p \epsilon_p (1 - \exp(-\lambda t_i)) \exp(-\lambda t_w) (1 - \exp(-\lambda t_m))} \quad /1/$$

where:

$N_p$  is the photopeak area of the characteristic gamma-ray of the residual nuclide;

$A_{gm}$  is the gram atomic weight of the target element;

$\lambda$  is the disintegration constant of the residual nuclide;

$\phi$  is the beam flux;

$W$  is the weight per unit area of the target foil;

$f_p$  is the fraction of characteristic gamma-rays emitted per decay of the residual nuclide;

$\epsilon_p$  is the photopeak efficiency of the gamma-ray;

and

$t_i$ ,  $t_w$  and  $t_c$  are the periods of irradiation, waiting and counting, respectively.

### 3. RESULTS AND DISCUSSION

The measured nuclidic cross sections for proton and  $^{12}\text{C}$ -ion induced reactions on  $^{55}\text{Mn}$ ,  $^{59}\text{Co}$ ,  $^{\text{nat}}\text{Ni}$  and  $^{\text{nat}}\text{Cu}$  are listed in Tables 3 and 4, respectively. The errors associated with the cross sections refer to counting statistics, detector efficiencies of gamma rays, target thicknesses and so on. The systematic uncertainties due to the beam flux, which were estimated to be about 15%, are not included in the quoted errors. Each yield was identified as being independent, I, or cumulative, C: the cumulative yields  $C^+$  and  $C^-$  represent the integrated isobaric cross section of neutron-deficient and neutron-excessive precursors, respectively.

The results from this experiment have been examined by the fitting procedure described in detail in our previous paper<sup>/11/</sup>. We assumed a smooth dependence of spallation cross sections  $\sigma(A, Z)$  on A and Z:

$$\ln [\sigma(A, Z)] = \sigma(A) + C(Z_p(A) - Z) \quad ; \quad /2/$$

$\sigma$ , C and  $Z_p$  define, respectively, the distribution of isobaric yields /mass-yield curve/, the fractional isobaric yields /charge-dispersion curve/ and the position of the maximum yield for a given A. The least-squares computer program FEDEF<sup>/12/</sup> was used to fit our data with the polynomial expression in A of varying order. Only independent yields /see Tables 3 and 4/ were taken into account.

For both sets of results the best fits of the fractional isobaric yields were obtained with the Gaussian form

$$\sigma_P = \exp \left\{ C [Z_p(A) - Z]^2 \right\} \quad /3/$$

with

$$Z_p(A) = b_1 A + b_2 A^2 \quad . \quad /4/$$

Table 3 Cross sections for proton-induced reactions

Product	$\sigma_{\text{Mn}}$ /mb/	$\sigma_{\text{Co}}$ /mb/	$\sigma_{\text{Ni}}$ /mb/	$\sigma_{\text{Cu}}$ /mb/
$^{57}\text{Ni}/\text{I}/$			$0.65 \pm 0.15$	$0.58 \pm 0.12$
$^{56}\text{Ni}/\text{I}/$			$0.20 \pm 0.07$	$0.13 \pm 0.06$
$^{60}\text{Co}/\text{I}/$				$8.30 \pm 0.41$
$^{58}\text{Co}/\text{I}/$		$18.91 \pm 0.36$		$19.85 \pm 0.92$
$^{57}\text{Co}/\text{C}^+ /$		$15.83 \pm 0.29$	$15.28 \pm 1.06$	$16.58 \pm 0.85$
$^{56}\text{Co}/\text{C}^+ /$		$7.20 \pm 0.54$	$5.00 \pm 0.52$	$4.97 \pm 0.28$
$^{55}\text{Co}/\text{C}^+ /$		$0.68 \pm 0.06$	$0.81 \pm 0.14$	$0.90 \pm 0.13$
$^{59}\text{Fe}/\text{C}^- /$				$1.23 \pm 0.18$
$^{52}\text{Fe}/\text{I}/$	$0.21 \pm 0.02$	$0.19 \pm 0.02$	$0.23 \pm 0.03$	$0.19 \pm 0.03$
$^{56}\text{Mn}/\text{C}^- /$		$2.44 \pm 0.12$	$2.37 \pm 0.41$	$2.31 \pm 0.22$
$^{54}\text{Mn}/\text{I}/$	$14.38 \pm 0.22$	$11.98 \pm 0.21$	$13.70 \pm 0.75$	$14.02 \pm 0.58$
$^{52}\text{Mn}/\text{I}/$	$5.29 \pm 0.11$	$5.36 \pm 0.10$	$5.92 \pm 0.38$	$5.55 \pm 0.19$
$^{51}\text{Cr}/\text{I}/$	$17.46 \pm 0.54$	$18.05 \pm 0.58$	$18.93 \pm 0.92$	$17.92 \pm 1.02$
$^{48}\text{Cr}/\text{I}/$	$0.41 \pm 0.04$	$0.33 \pm 0.03$	$0.16 \pm 0.04$	$0.35 \pm 0.04$
$^{48}\text{V}/\text{C}^+ /$	$11.88 \pm 0.38$	$10.93 \pm 0.39$	$9.88 \pm 0.45$	$9.44 \pm 0.27$
$^{48}\text{Sc}/\text{I}/$	$0.52 \pm 0.02$	$0.58 \pm 0.03$	$0.69 \pm 0.09$	$0.68 \pm 0.08$
$^{47}\text{Sc}/\text{I}/$	$2.15 \pm 0.12$	$2.22 \pm 0.14$	$2.06 \pm 0.32$	$2.38 \pm 0.14$
$^{46}\text{Sc}/\text{I}/$	$5.71 \pm 0.32$	$5.99 \pm 0.33$	$6.85 \pm 0.58$	$6.05 \pm 0.25$
$^{44}\text{Sc}^{\text{m}}/\text{I}/$	$3.99 \pm 0.13$	$4.35 \pm 0.12$	$4.59 \pm 0.37$	$5.17 \pm 0.28$
$^{44}\text{Sc}/\text{I}/$	$3.08 \pm 0.16$	$3.94 \pm 0.18$	$4.06 \pm 0.38$	$3.86 \pm 0.25$
$^{43}\text{Sc}/\text{C}^+ /$	$2.05 \pm 0.08$	$3.11 \pm 0.10$	$3.82 \pm 0.31$	$3.76 \pm 0.32$
$^{43}\text{K}/\text{C}^- /$	$1.23 \pm 0.06$	$1.20 \pm 0.06$	$1.64 \pm 0.22$	$1.33 \pm 0.16$
$^{42}\text{K}/\text{I}/$	$2.90 \pm 0.17$	$3.07 \pm 0.16$	$2.59 \pm 0.21$	$2.99 \pm 0.61$
$^{28}\text{Mg}/\text{C}^- /$	$0.14 \pm 0.02$	$0.37 \pm 0.04$	$0.51 \pm 0.07$	$0.55 \pm 0.07$
$^{24}\text{Mg}/\text{C}^- /$	$3.15 \pm 0.10$	$3.29 \pm 0.11$	$3.06 \pm 0.19$	$3.50 \pm 0.18$

Table 4 Cross sections for  $^{12}\text{C}$ -ion-induced reactions

Product	$\sigma_{\text{Mn}}$ /mb/	$\sigma_{\text{Co}}$ /mb/	$\sigma_{\text{Ni}}$ /mb/	$\sigma_{\text{Cu}}$ /mb/
$^{65}\text{Zn}/\text{I}/$	$5.31 \pm 1.10$	$4.08 \pm 0.96$	$4.63 \pm 0.97$	$4.94 \pm 1.05$
$^{61}\text{Cu}/\text{C}^+ /$			$22.77 \pm 4.08$	$23.01 \pm 2.26$
$^{57}\text{Ni}/\text{I}/$	$1.54 \pm 0.48$	$1.27 \pm 0.53$	$1.30 \pm 0.42$	$1.33 \pm 0.62$
$^{56}\text{Ni}/\text{I}/$	$0.17 \pm 0.12$	$0.30 \pm 0.10$	$0.25 \pm 0.13$	$0.29 \pm 0.18$
$^{60}\text{Co}/\text{I}/$	$32.49 \pm 4.96$	$28.79 \pm 4.72$	$30.76 \pm 4.79$	$31.87 \pm 5.11$
$^{58}\text{Co}/\text{I}/$	$52.83 \pm 7.21$	$58.22 \pm 8.85$	$55.92 \pm 7.86$	$56.54 \pm 8.27$
$^{57}\text{Co}/\text{C}^+ /$	$43.60 \pm 5.12$	$46.13 \pm 5.41$	$41.05 \pm 5.19$	$42.69 \pm 5.43$
$^{56}\text{Co}/\text{C}^+ /$	$11.72 \pm 1.95$	$15.65 \pm 2.24$	$13.74 \pm 1.94$	$13.25 \pm 2.07$
$^{55}\text{Co}/\text{C}^+ /$		$1.83 \pm 0.85$	$2.10 \pm 0.66$	$2.32 \pm 0.89$
$^{59}\text{Fe}/\text{C}^- /$	$3.55 \pm 1.03$	$4.11 \pm 1.07$	$3.17 \pm 0.99$	$2.86 \pm 0.94$
$^{52}\text{Fe}/\text{I}/$	$0.21 \pm 0.07$	$0.39 \pm 0.16$	$0.35 \pm 0.13$	$0.33 \pm 0.14$
$^{56}\text{Mn}/\text{C}^- /$	$6.26 \pm 1.04$		$4.80 \pm 0.98$	$5.28 \pm 1.02$
$^{54}\text{Mn}/\text{I}/$	$27.85 \pm 2.29$	$31.14 \pm 3.08$	$28.33 \pm 2.11$	$29.11 \pm 2.67$
$^{52}\text{Mn}/\text{I}/$	$10.38 \pm 1.07$	$11.92 \pm 1.15$	$11.17 \pm 1.05$	$10.80 \pm 1.06$
$^{51}\text{Cr}/\text{I}/$	$42.07 \pm 5.00$	$43.05 \pm 4.97$	$44.42 \pm 5.14$	$41.50 \pm 4.88$
$^{48}\text{Cr}/\text{I}/$	$0.81 \pm 0.21$	$0.59 \pm 0.19$	$0.68 \pm 0.25$	$0.73 \pm 0.23$
$^{48}\text{V}/\text{C}^+ /$	$20.58 \pm 2.06$	$18.70 \pm 1.41$	$19.93 \pm 1.37$	$20.24 \pm 1.41$
$^{48}\text{Sc}/\text{I}/$	$2.00 \pm 0.51$	$2.08 \pm 0.59$	$1.85 \pm 0.49$	$1.93 \pm 0.57$
$^{47}\text{Sc}/\text{I}/$	$4.83 \pm 0.73$	$5.37 \pm 0.92$	$5.35 \pm 0.85$	$5.42 \pm 0.72$
$^{46}\text{Sc}/\text{I}/$	$14.02 \pm 1.95$	$12.66 \pm 1.48$	$11.89 \pm 1.69$	$13.05 \pm 1.74$
$^{44}\text{Sc}^{\text{m}}/\text{I}/$	$11.44 \pm 1.49$	$9.87 \pm 1.13$	$12.05 \pm 1.37$	$13.35 \pm 1.98$
$^{44}\text{Sc}/\text{I}/$	$7.35 \pm 1.64$	$6.52 \pm 1.65$	$8.14 \pm 1.84$	$7.99 \pm 1.39$
$^{43}\text{Sc}/\text{C}^+ /$	$8.10 \pm 1.26$	$6.94 \pm 1.18$	$7.88 \pm 1.13$	$7.25 \pm 1.35$
$^{43}\text{K}/\text{C}^- /$	$1.92 \pm 0.50$	$2.71 \pm 0.76$	$2.36 \pm 0.64$	$2.42 \pm 0.63$
$^{42}\text{K}/\text{I}/$	$6.15 \pm 1.72$	$5.83 \pm 2.07$	$4.71 \pm 1.92$	$5.37 \pm 1.97$
$^{28}\text{Mg}/\text{C}^- /$	$0.42 \pm 0.07$	$0.95 \pm 0.19$	$1.37 \pm 0.38$	$1.56 \pm 0.40$
$^{24}\text{Na}/\text{C}^- /$	$10.23 \pm 1.19$	$11.06 \pm 1.42$	$8.93 \pm 1.22$	$9.12 \pm 1.26$

No significant deviations of the yields of spallation products for all medium targets used in the present experiment from this charge dispersion curve were obtained. The FWHM of the Gaussian curve was equal to about  $-1.2$ . The values of  $Z_p$  for a given A in a given mass region of the spallation products are independent of the nature of the projectile: the parameters  $b_1$  were found to be in the range from 0.47 to 0.48 and  $b_2$  ranged from  $-2.5 \times 10^{-4}$  to  $-4.3 \times 10^{-4}$ . The charge dispersion curves obtained from this fitting procedure are shown in Fig.2. Here, the upper curves and open points are for  $^{12}\text{C}$ -ions, the lower curves and filled points are for protons. The appropriate curves are displaced vertically by a factor of 10 for the display purposes. As can be seen from this figure, the agreement between the charge distributions for both projectiles is evident.

While the charge dispersions were refined, the mass-yield distributions  $\sigma_A$  were also examined for each of the appropriate data sets. The best fits of the mass yields were obtained with the quadratic form of A

$$\sigma_A = \exp \{ a_0 + a_1 A + a_2 A^2 \} \quad /5/$$

The best fitting parameters were used to calculate missing yields in addition to the observed cross sections: an error of 20% of the missing yields was assumed. The resulting mass-yield distributions are displayed in Fig.3. The fraction of the isobaric cross section determined experimentally is denoted by different symbols: they are filled for a contribution of  $> 50\%$  of the observed cross section and open for 20-50%. The solid lines are the least-squares

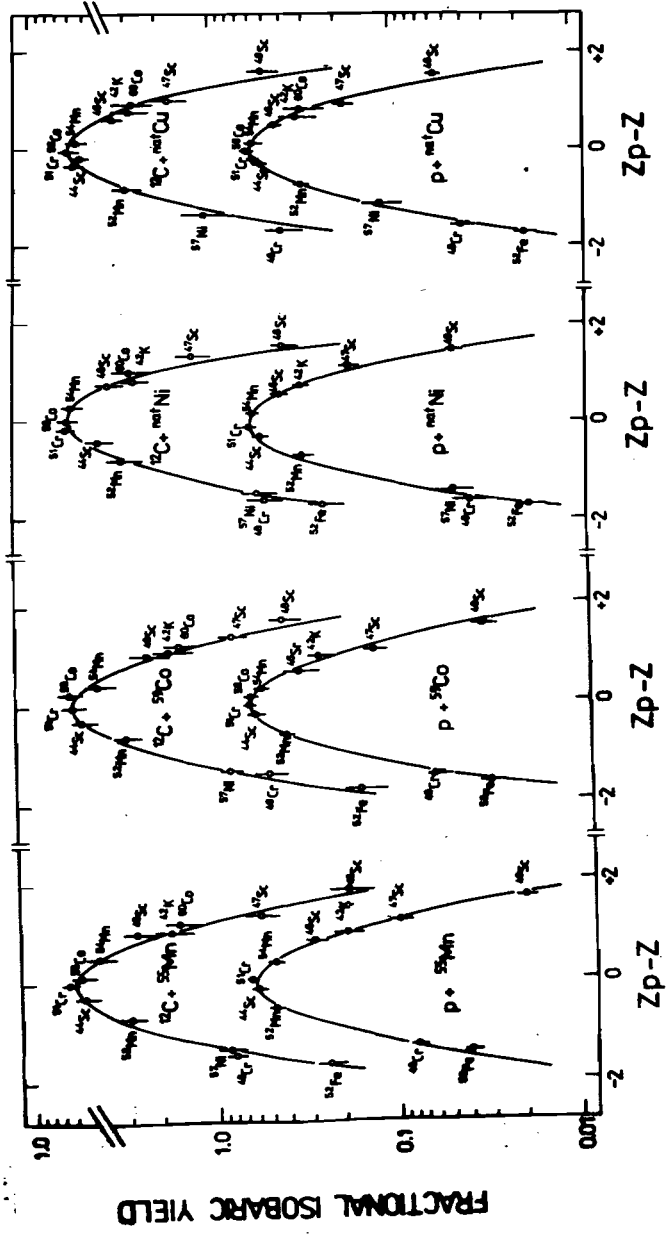


Fig.2. Comparison of the fractional isobaric yields / charge curves / for the  $^{12}\text{C}$ -ion- and proton-induced reactions.

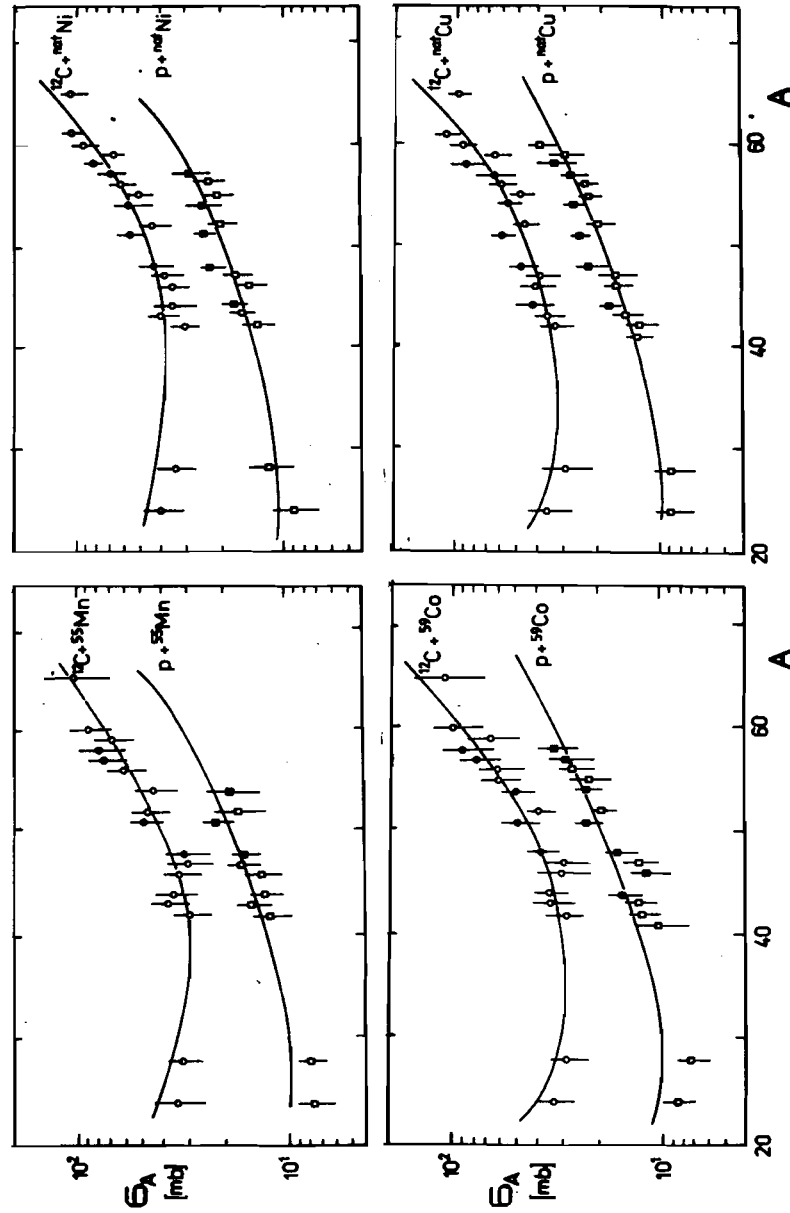


Fig.3. The mass-yield distributions of radioactive residues of 3.65 AGeV  $^{12}\text{C}$ -ions and 3.65 GeV protons with  $^{55}\text{Mn}$ ,  $^{59}\text{Co}$ ,  $^{63}\text{Ni}$  and  $^{65}\text{Cu}$ . The points are the experimental contributions obtained from the fitting procedure described in the text. The symbols are filled for the observed products accounting > 50% of the total yield and open for 20-50%.

fits to all the data in this mass region. The agreement with the experimental points is reasonable. The similarities between the mass-yield distributions for 3.65 AGeV  $^{12}\text{C}$ -ions and 3.65 GeV protons observed in the spallation of medium target nuclei / $^{55}\text{Mn}$ ,  $^{59}\text{Co}$ ,  $\text{natNi}$  and  $\text{natCu}$ / show experimental evidence for the factorization. The appropriate ratios of the isobaric cross sections  $\sigma_A$  /plotted in Fig.3/ were found to be constant for a wide range of spallation products. The observed relative factorization ratios  $\gamma_{12\text{C}}/\gamma_p$  for all target nuclei used in the present experiment were about  $2.4 \pm 0.5$ . This is consistent with the ratio of the total cross sections of monitoring reactions  $^{27}\text{Al}/^{12}\text{C}, X/^{24}\text{Na}$  and  $^{27}\text{Al}/^{12}\text{C}, X/^{24}\text{Na}$ .

To test the limiting fragmentation, we compared the present data with the previous spallation results at other energies. The comparison of our  $p+^{59}\text{Co}$  results at 3.65 GeV with the previous data of Katcoff et al. /<sup>13/</sup> at 11.5, 200 and 300 GeV is made in Table 5. It appears from the first column of this table that for  $^{59}\text{Co}$  the spallation cross sections for all the products measured at 3.65 GeV are very nearly the same as at 11.5 GeV; the mean cross section ratio  $\sigma_{3.65}/\sigma_{11.5}$  for all measured products is  $0.96 \pm 0.15$ . The data of Katcoff et al. /<sup>13/</sup> at 11.5 GeV were related to the cross section of  $^{27}\text{Al}/p, X/^{24}\text{Na}$  8.3 mb. It should be noted that the mean ratios  $\sigma_{200}/\sigma_{11.5}$  and  $\sigma_{300}/\sigma_{11.5}$  determined in paper /<sup>13/</sup> are  $0.95 \pm 0.06$  and  $1.02 \pm 0.05$ , respectively. Thus, it can be summarized that cross sections of products from the spallation of cobalt by high-energy protons are energy independent over the energy range from 3.65 to 300 GeV. In Table 6 we compare our  $^{12}\text{C}+\text{natCu}$  results at

Table 5 Cross section ratios  $\sigma_{3.65}/\sigma_{11.5}$ ,  $\sigma_{200}/\sigma_{11.5}$  and  $\sigma_{300}/\sigma_{11.5}$  of radionuclides produced from  $^{59}\text{Co}$  by 3.65 GeV /present results/, 200, 300 and 11.5 GeV protons /<sup>13/</sup>

Nuclide	$\sigma_{3.65}/\sigma_{11.5}$	$\sigma_{200}/\sigma_{11.5}$	$\sigma_{300}/\sigma_{11.5}$
$^{58}\text{Co}$	$0.93 \pm 0.16$	$0.95 \pm 0.12$	$1.13 \pm 0.10$
$^{57}\text{Co}$	$0.83 \pm 0.16$	$0.87 \pm 0.10$	$1.10 \pm 0.12$
$^{56}\text{Co}$	$1.46 \pm 0.23$	$0.95 \pm 0.12$	$1.04 \pm 0.10$
$^{55}\text{Co}$	$1.01 \pm 0.26$	$1.03 \pm 0.34$	$1.02 \pm 0.17$
$^{54}\text{Mn}$	$0.65 \pm 0.08$	$0.92 \pm 0.13$	$1.06 \pm 0.17$
$^{52}\text{Mn}$	$1.03 \pm 0.11$	$0.90 \pm 0.13$	$1.04 \pm 0.12$
$^{51}\text{Cr}$	$0.89 \pm 0.11$	$0.99 \pm 0.14$	$1.01 \pm 0.11$
$^{48}\text{Cr}$	$1.22 \pm 0.20$	$0.92 \pm 0.11$	$0.93 \pm 0.08$
$^{48}\text{V}$	$1.20 \pm 0.14$	$0.88 \pm 0.11$	$1.00 \pm 0.09$
$^{48}\text{Sc}$	$1.00 \pm 0.26$		$0.95 \pm 0.12$
$^{47}\text{Sc}$	$0.85 \pm 0.12$	$0.96 \pm 0.12$	$1.05 \pm 0.09$
$^{46}\text{Sc}$	$0.92 \pm 0.13$	$0.99 \pm 0.12$	$1.01 \pm 0.09$
$^{43}\text{K}$	$0.97 \pm 0.13$	$0.93 \pm 0.16$	$0.98 \pm 0.13$
$^{42}\text{K}$	$0.82 \pm 0.15$	$0.95 \pm 0.16$	$0.85 \pm 0.12$
$^{28}\text{Mg}$	$0.76 \pm 0.10$	$1.00 \pm 0.17$	$1.06 \pm 0.11$
$^{24}\text{Na}$	$0.77 \pm 0.06$	$0.96 \pm 0.08$	$1.02 \pm 0.09$

3.65 AGeV with the previous data at 1.54 AGeV /<sup>14/</sup> and 2.1 AGeV /<sup>15/</sup>. Unfortunately, there is lack of sufficient data in a wide range of spallation products at 1.54 AGeV /<sup>14/</sup>. Nevertheless, the obtained ratios  $\sigma_{3.65}/\sigma_{1.54}$  within errors fluctuate about unity. On the other hand, the mean ratio  $\sigma_{3.65}/\sigma_{2.1}$  of measured 26 cross sections  $1.06 \pm 0.30$



gives overwhelming evidence that the spallation cross sections are constant over the energy range from 2.1 to 3.65 AGeV.

Table 6 Comparison of the  $^{12}\text{C} + \text{nat}\text{Cu}$  spallation cross sections at 3.65 AGeV with previous data at 1.54 AGeV<sup>/14/</sup> and 2.1 AGeV<sup>/15/</sup>

Nuclide	$\sigma_{3.65}/\sigma_{1.54}$	$\sigma_{3.65}/\sigma_{2.1}$
$^{65}\text{Zn}$		$1.00 \pm 0.27$
$^{61}\text{Cu}$		$0.75 \pm 0.11$
$^{57}\text{Ni}$		$0.88 \pm 0.45$
$^{56}\text{Ni}$		$1.21 \pm 0.56$
$^{60}\text{Co}$		$1.08 \pm 0.21$
$^{58}\text{Co}$		$0.92 \pm 0.15$
$^{57}\text{Co}$		$0.90 \pm 0.13$
$^{56}\text{Co}$		$0.97 \pm 0.15$
$^{55}\text{Co}$		$1.01 \pm 0.43$
$^{59}\text{Fe}$		$0.63 \pm 0.22$
$^{52}\text{Fe}$		$1.18 \pm 0.68$
$^{56}\text{Mn}$		$0.69 \pm 0.24$
$^{54}\text{Mn}$		$0.89 \pm 0.10$
$^{52}\text{Mn}$	$1.00 \pm 0.13$	$0.91 \pm 0.10$
$^{51}\text{Cr}$		$1.17 \pm 0.15$
$^{48}\text{Cr}$		$1.38 \pm 0.54$
$^{48}\text{V}$	$1.25 \pm 0.17$	$1.20 \pm 0.10$
$^{48}\text{Sc}$	$1.58 \pm 0.63$	$1.86 \pm 0.63$
$^{47}\text{Sc}$		$1.24 \pm 0.21$
$^{46}\text{Sc}$		$1.19 \pm 0.18$
$^{44}\text{Sc}$		$1.07 \pm 0.27$
$^{43}\text{Sc}$		$0.99 \pm 0.35$
$^{43}\text{K}$		$1.03 \pm 0.30$
$^{42}\text{K}$	$0.78 \pm 0.42$	$0.77 \pm 0.34$
$^{28}\text{Mg}$	$1.50 \pm 0.51$	$1.63 \pm 0.57$
$^{24}\text{Na}$	$0.94 \pm 0.16$	$0.98 \pm 0.17$

#### 4. CONCLUSIONS

Our experimental data provide new information on the spallation of medium target nuclei by high-energy protons and  $^{12}\text{C}$ -ions.

The fractional isobaric yields were found to be the same for both sets of spallation products. No significant deviations from the Gaussian charge dispersion were obtained. The values of the most probable charge  $Z_p$  for a given A in the whole mass range of spallation products were found to be independent of the projectile.

The similarity of the mass-yield distributions from the reactions  $^{12}\text{C} + ^{55}\text{Mn}$ ,  $^{59}\text{Co}$ ,  $\text{nat}\text{Ni}$ ,  $\text{nat}\text{Cu}$  and  $p + ^{55}\text{Mn}$ ,  $^{59}\text{Co}$ ,  $\text{nat}\text{Ni}$ ,  $\text{nat}\text{Cu}$ , respectively, at the same bombarding energy 3.65 AGeV proved the validity of the factorization hypothesis. Evidence for limiting fragmentation was demonstrated by the comparison of our proton and  $^{12}\text{C}$ -ion results with the previous data at other energies.

#### References

- /1/ Goldhaber A.S., Heckman H.: Annu.Rev.Nucl.Part.Sci. 28 /1978/ and references cited here; Fredriksson S., Eilam G., Berlaud G., Bergström L.: Phys.Rep. 144 /1987/ 187 and references cited here.
- /2/ Barashenkov V.S., Toneev V.D.: Interactions of High-Energy Particles and Atomic Nuclei with Nuclei, Atomizdat, Moscow, 1972.
- /3/ Bertini H.W., Guthrie M.P.: Nucl.Phys. A 169 /1971/ 670.
- /4/ Yariv Y., Fraenkel Z.: Phys.Rev. C 20 /1979/ 2227.
- /5/ Bowman J.D., Swiatecki W.J., Tsang C.F.: LBL Report, LBL-2908, 1973.

- /6/ Boggild H., Ferbel T.: Annu.Rev.Nucl.Sci. 24 /1974/ 451.
- /7/ Damdinsuren C., Duka-Zolyómi A., Dyachenko V.M., Kliman J., Kozma P., Tumenemberel B.: JINR Report P1-87-932, Dubna, 1987.
- /8/ Tumenemberel B.: JINR Report P10-87-152, Dubna, 1987.
- /9/ Reus U., Westmeier W.: Atomic and Nuclear Data Tables 29, /1983/ 1-493.
- /10/ Rama Rao J., Mohan Rao A.V., Mukherjee S., Upadhyay R., Singh N.L., Agarwall S., Chaturvedi L., Singh P.P.: J.Phys.G.:Nucl.Phys. 13 /1987/ 535.
- /11/ Kozma P., Kliman J.: Czech.J.Phys.B, to be published; and JINR Report E1-86-606, Dubna, 1986.
- /12/ Kozma P., Kozmová J., Streit E., Hnatowicz V.: Report JINR E10-86-430, Dubna, 1986.
- /13/ Katcoff S., Kaufman S.B., Steinberg E.P., Weisfield M.W., Wilkins B.D.: Phys.Rev.Lett. 30 /1973/ 1221.
- /14/ Cole G.D., Porile N.T.: Phys.Rev. C 24 /1981/ 2038.
- /15/ Cumming J.B., Haustein P.E., Stoenner R.W.: Phys.Rev. C 14 /1976/ 1554.

Received by Publishing Department  
on April 14, 1988.

Козма П., Тумэндэмбэрэл Б., Чултэм Д.

E1-88-244

Взаимодействие снарядов высоких энергий со средними и тяжелыми ядрами. Обдирка ядер  $^{55}\text{Mn}$ ,  $^{59}\text{Co}$ ,  $^{nat}\text{Ni}$  и  $^{nat}\text{Cu}$  ядрами  $^{12}\text{C}$  и протонами с энергией 3.65 ГэВ/нуклон

Ядерные реакции, вызванные ядрами  $^{12}\text{C}$  и протонами с энергией 3.65 ГэВ/нуклон на ядрах  $^{55}\text{Mn}$ ,  $^{59}\text{Co}$ ,  $^{nat}\text{Ni}$ ,  $^{nat}\text{Cu}$  были исследованы посредством методики наведенной активности и гамма-спектроскопии с Ge(Li) детекторами. Зарядовые дисперсии и массовые распределения радиоактивных остатков были получены параметризацией экспериментальных сечений. Дискуссия результатов этого и других радиохимических экспериментов проводится в рамках предельной фрагментации и факторизации.

Работа выполнена в Лаборатории высоких энергий ОИЯИ.

Препринт Объединенного института ядерных исследований. Дубна 1988

Kozma P., Tumenemberel B., Chultem D.

E1-88-244

Nuclear Reactions of Medium and Heavy Target Nuclei with High-Energy Projectiles. Spallation of  $^{55}\text{Mn}$ ,  $^{59}\text{Co}$ ,  $^{nat}\text{Ni}$  and  $^{nat}\text{Cu}$  by 3.65 AGeV  $^{12}\text{C}$ -ions and 3.65 GeV Protons

Nuclear reactions induced by 3.65 AGeV  $^{12}\text{C}$ -ions and 3.65 GeV protons in target elements  $^{55}\text{Mn}$ ,  $^{59}\text{Co}$ ,  $^{nat}\text{Ni}$  and  $^{nat}\text{Cu}$  were investigated by using the foil stack activation technique and Ge(Li) gamma-ray spectroscopy. Charge dispersions and mass-yield distributions of radioactive residues were obtained from the parametrization of measured spallation cross sections. The discussion of results from this and other radiochemical experiments with high-energy protons and  $^{12}\text{C}$ -ions with complex nuclei is presented in terms of the concepts of limiting fragmentation and factorization.

The investigation has been performed at the Laboratory of High Energies, JINR.

Preprint of the Joint Institute for Nuclear Research. Dubna 1988